CHAPTER 1

Integral Equation Formulations

Elliptic PDEs such as the Laplace and the Helmholtz equations are well known as the mathematical equations that arise when modeling problems such as electrostatics, gravitation, time harmonic wave propagation problems, and so on. In this chapter, we will see that many problems that can be modeled with elliptic PDEs, can alternatively be formulated as integral equations. Such a formulation is in many environments very attractive from the point of view of numerical work. The most obvious advantage of methods based on integral equations arises for problems involving constant coefficient differential operators (i.e. physical properties such as conductivity or wave speed remain constant throughout the domains), and no body loads. In this situation, the integral equation can be formulated on the *boundary* of the domain only, which leads to a reduction in dimension. Another important benefit is that an integral operator is in certain ways a more benign mathematical object than a differential operator, which enables us to derive numerical methods of exceptional stability and accuracy.

We will in this chapter illustrate some of the possibilities that integral equation formulations offer by looking at several simple examples.

1.1. Reducing the dimension of the computational domain

In this chapter, we consider a simple elliptic PDE formulated on a two-dimensional domain Ω in the plane. We will show how a Boundary Integral Equation (BIE) formulation can be used to construct a mathematical model that is defined only on the boundary Γ of the domain. This means that when we discretize the equation, we need only discretize a 1D object.

As a model problem, we consider the Laplace equation with Dirichlet boundary data

$$\begin{cases} -\Delta u(\boldsymbol{x}) = 0 & \text{for } \boldsymbol{x} \in \Omega, \\ u(\boldsymbol{x}) = f(\boldsymbol{x}) & \text{for } \boldsymbol{x} \in \Gamma, \end{cases} \tag{1.1}$$

where Ω is a simply connected open set in $\mathbb{R}^2$ with smooth boundary $\Gamma = \partial\Omega$. Our objective is to rewrite (1.1) as an equation involving only quantities that are defined on the boundary Γ. To this end, we seek a solution of the form

$$u(\boldsymbol{x}) = \int_\Gamma \phi(\boldsymbol{x} - \boldsymbol{y})\, \sigma(\boldsymbol{y})\, ds(\boldsymbol{y}), \qquad \boldsymbol{x} \in \Omega, \tag{1.2}$$

where ϕ is the fundamental solution of the Laplace operator

$$\phi(\boldsymbol{x}) = -\frac{1}{2\pi} \log |\boldsymbol{x}|,$$

and where σ is a function that we will need to determine. Any function u defined via (1.2) satisfies $-\Delta u(\boldsymbol{x}) = 0$ when $\boldsymbol{x} \in \Omega$. This is a direct consequence of the fact that ϕ is harmonic away from the origin, and so u is simply a superposition of harmonic functions. This leaves us with the question of whether the boundary condition is satisfied. It turns out that for any reasonably nice function σ, the function u defined by (1.2) is continuous on the closed domain $\bar{\Omega}$, so the boundary condition is satisfied if and only if

$$\int_\Gamma \phi(\boldsymbol{x} - \boldsymbol{y})\, \sigma(\boldsymbol{y})\, ds(\boldsymbol{y}) = f(\boldsymbol{x}), \qquad \boldsymbol{x} \in \Gamma. \tag{1.3}$$

The equation (1.3) is now a BIE formulation of (1.1), and we see that we have succeeded in rewriting an equation defined on the 2D domain Ω as an equation defined on the 1D domain Γ. The importance of this from the point of view of numerical work is that far fewer degrees of freedom are required to discretize a one-dimensional curve such as Γ, than to discretize a two-dimensional domain such as Ω to a comparable resolution. To be precise, if our grid spacing is h, then as $h \to 0$, we need $O(h^{-1})$ points to discretize Γ, and $O(h^{-2})$ points to discretize Ω.

The mathematical reasoning in the previous paragraph is fast and loose, and we leave the details to more mathematically rigorous texts such as [**7, 8**]. However, it is perhaps worthwhile to take a moment to think about what steps would be needed. First, we would need to verify that the equation (1.3) actually has a solution. As long as f is not too irregular, this is not difficult to do, but it does require some analysis. Once we have established that a solution σ exists and has some regularity (say integrability on the boundary), then it is a relatively simple matter to first prove that it is permissible to differentiate (1.2) under the integral

$$-\Delta_{\boldsymbol{x}} u(\boldsymbol{x}) = \int_\Gamma \underbrace{-\Delta_{\boldsymbol{x}} \phi(\boldsymbol{x}-\boldsymbol{y})}_{=0}\, \sigma(\boldsymbol{y})\, ds(\boldsymbol{y}) = 0, \tag{1.4}$$

and then that the function u defined by (1.2) is continuous on the closed domain $\bar{\Omega}$, or in other words, that

$$\lim_{\boldsymbol{x}' \to \boldsymbol{x}, \boldsymbol{x}' \in \Omega} \int_\Gamma \phi(\boldsymbol{x}'-\boldsymbol{y})\, \sigma(\boldsymbol{y})\, ds(\boldsymbol{y}) = \int_\Gamma \phi(\boldsymbol{x}-\boldsymbol{y})\, \sigma(\boldsymbol{y})\, ds(\boldsymbol{y}). \tag{1.5}$$

For future reference, we define the *single layer operator* S via

$$[S\sigma](\boldsymbol{x}) = \int_\Gamma \phi(\boldsymbol{x}-\boldsymbol{y})\, \sigma(\boldsymbol{y})\, ds(\boldsymbol{y}) = \int_\Gamma -\frac{1}{2\pi} \log|\boldsymbol{x}-\boldsymbol{y}|\, \sigma(\boldsymbol{y})\, ds(\boldsymbol{y}), \qquad \text{where } \boldsymbol{x} \in \mathbb{R}^2.$$

1.2. Obtaining a well-conditioned mathematical equation

In Section 1.1, we showed how an integral equation formulation can be used to reduce the dimension of the domain to be discretized. In this section, we will explore how similar techniques can be used to obtain linear systems that are well-conditioned. In this discussion, let us first recall that if we discretize the BVP (1.1) directly, then the resulting linear system will have a condition number that typically scales as $O(h^{-2})$ as the grid spacing h tends to zero. The simple BIE (1.3) that we derived in Section 1.1 leads to a linear system with typical condition number of $O(h^{-1})$. This represents a meaningful reduction in ill-conditioning, but we can do much better: It turns out that we can find a BIE whose condition number *converges to a finite number* as $h \to 0$. (Moreover, the finite number often ends up being not much larger than one.) To describe how this works, let us look for a solution to (1.1) that takes the form

$$u(\boldsymbol{x}) = \int_\Gamma d(\boldsymbol{x}, \boldsymbol{y})\, \sigma(\boldsymbol{y})\, ds(\boldsymbol{y}), \qquad \boldsymbol{x} \in \Omega, \tag{1.6}$$

where $d(\boldsymbol{x}, \boldsymbol{y})$ is a kernel function that is defined as the normal derivative to the fundamental solution ϕ at the point $\boldsymbol{y}$. To be precise, for $\boldsymbol{y} \in \Gamma$, we let $\boldsymbol{n}(\boldsymbol{y})$ denote the normal of Γ at $\boldsymbol{y}$. Then

$$d(\boldsymbol{x}, \boldsymbol{y}) = \boldsymbol{n}(\boldsymbol{y}) \cdot \nabla_{\boldsymbol{y}} \phi(\boldsymbol{x}-\boldsymbol{y}) = -\frac{\boldsymbol{n}(\boldsymbol{y}) \cdot (\boldsymbol{x}-\boldsymbol{y})}{2\pi|\boldsymbol{x}-\boldsymbol{y}|^2}. \tag{1.7}$$

Using an argument that is entirely analogous to the argument in Section 1.1, one can easily demonstrate that the potential u defined by (1.6) is harmonic in Ω. However, the kernel function $d(\boldsymbol{x}, \boldsymbol{y})$ has a stronger singularity as $\boldsymbol{x} \to \boldsymbol{y}$, which means that as we take the limit of $u(\boldsymbol{x})$ as $\boldsymbol{x}$ approaches the boundary, an additional term arises. The exact statement is that for any $\boldsymbol{x} \in \Gamma$, we have [ref??]

$$\lim_{\boldsymbol{x}' \to \boldsymbol{x}, \boldsymbol{x}' \in \Omega} \int_\Gamma d(\boldsymbol{x}', \boldsymbol{y})\, \sigma(\boldsymbol{y})\, ds(\boldsymbol{y}) = -\frac{1}{2}\sigma(\boldsymbol{x}) + \int_\Gamma d(\boldsymbol{x}, \boldsymbol{y})\, \sigma(\boldsymbol{y})\, ds(\boldsymbol{y}). \tag{1.8}$$

This means that the BIE we need to solve now takes the form

$$-\frac{1}{2}\sigma(\boldsymbol{x}) + \int_\Gamma d(\boldsymbol{x},\boldsymbol{y})\,\sigma(\boldsymbol{y})\,ds(\boldsymbol{y}) = f(\boldsymbol{x}), \qquad \boldsymbol{x}\in\Gamma. \tag{1.9}$$

Looking at (1.9), and remembering the definition of d in (1.7), we may worry about the singularity that appears to be of strength $O(|\boldsymbol{x}-\boldsymbol{y}|^{-1})$ as $\boldsymbol{y}\to\boldsymbol{x}$. But since $\boldsymbol{y}$ approaches $\boldsymbol{x}$ *along the contour* Γ, the two vectors $\boldsymbol{n}(\boldsymbol{y})$ and $\boldsymbol{x}-\boldsymbol{y}$ become orthogonal as $\boldsymbol{y}$ approaches $\boldsymbol{x}$. In consequence, $\boldsymbol{n}(\boldsymbol{y})\cdot(\boldsymbol{x}-\boldsymbol{y}) = O(|\boldsymbol{y}-\boldsymbol{x}|^2)$, and so $d(\boldsymbol{x},\boldsymbol{y})$ converges to a finite limit as $\boldsymbol{y}\to\boldsymbol{x}$. In fact, one can prove that for a fixed $\boldsymbol{x}\in\Gamma$, the function $\boldsymbol{y}\mapsto d(\boldsymbol{x},\boldsymbol{y})$ is C^∞, cf. Remark 2.2. For future reference, let us define the *double layer operator* D via

$$[D\sigma](\boldsymbol{x}) = \int_\Gamma d(\boldsymbol{x},\boldsymbol{y})\,\sigma(\boldsymbol{y})\,ds(\boldsymbol{y}) = \int_\Gamma \frac{\boldsymbol{n}(\boldsymbol{y})\cdot(\boldsymbol{x}-\boldsymbol{y})}{2\pi\,|\boldsymbol{x}-\boldsymbol{y}|^2}\,\sigma(\boldsymbol{y})\,ds(\boldsymbol{y}). \tag{1.10}$$

At this point, it may seem as if we have taken a path to converting the PDE (1.1) into the BIE (1.9) that is unnecessarily cumbersome. But there is a purpose to this, which is that the integral equation (1.9) is what is called a *Fredholm equation of the second kind*. This means that while the equation is a continuum equation that acts on an infinite dimension space, it in many ways behave very much like a simple finite dimensional linear system. To be slightly more precise, the equation (1.9) takes the form

$$\left(-\frac{1}{2}I + D\right)\sigma = f,$$

where D is the operator defined in (1.10). Let us assume that Γ is smooth, and then view D as an operator from $L^2(\Gamma)$ to itself. Then the operator D is *compact*, which is to say that to any finite precision ε, it behaves like a finite dimensional operator. So the operator $-\frac{1}{2}I + D$ is for practical purposes a finite dimensional perturbation to the scaling operator $-\frac{1}{2}I$, which makes $-\frac{1}{2}I + D$ a very benign mathematical object.

Practically speaking, an essential benefit of finding a mathematical formulation in the form of a Fredholm equation of the second kind is that when we discretize it to obtain a linear system $\mathbf{A}\mathbf{x} = \mathbf{b}$, then the condition number of the matrix $\mathbf{A}$ converges to a finite number as the number of discretization points N tends to infinity. Moreover, since the singular values of the discretized operator has only a single cluster point at $-1/2$, iterative solvers tend to converge very rapidly. In particular, the number of iterations required does not increase as the number of discretization nodes increases.

1.3. External domains and boundary conditions "at infinity" for the Laplace equation

Let us next consider a boundary value problem that is defined on a domain Ω that is *exterior* to some smooth finite contour Γ is the plane. To be precise, we will for a given function f on Γ consider the boundary value problem

$$\begin{cases} -\Delta u(\boldsymbol{x}) = 0, & \text{for } \boldsymbol{x}\in\Omega, \\ u(\boldsymbol{x}) = f(\boldsymbol{x}), & \text{for } \boldsymbol{x}\in\Gamma, \\ \exists Q\in\mathbb{R}:\ \lim\limits_{|\boldsymbol{x}|\to\infty}\left(u(\boldsymbol{x}) - \dfrac{Q}{2\pi}\log|\boldsymbol{x}|\right) = 0. \end{cases} \tag{1.11}$$

Note that in (1.11), we have a standard Dirichlet boundary condition on Γ, and the third line represents a limit on how rapidly a solution may grow at infinity. This last line is necessary to ensure that the equation is well-posed and has a unique solution.[1]

[1]For a reader unfamiliar with exterior problems, it is perhaps helpful to consider what happens to (1.11) for the case where Γ is the circle $\Gamma = \{\boldsymbol{x}\in\mathbb{R}^2 : |\boldsymbol{x}| = R\}$. In this case, a standard solution technique is to work with polar coordinates $\boldsymbol{x} = r(\cos\theta,\,\sin\theta)$, and to expand f as a Fourier series $f(\theta) = a_0 + \sum_{n=1}^\infty\big(a_n\cos(n\theta) + b_n\sin(n\theta)\big)$. One physically meaningful solution to (1.11) is then $u(r,\theta) = a_0'\log(r) + \sum_{n=1}^\infty r^{-n}\big(a_n'\cos(n\theta) + b_n'\sin(n\theta)\big)$ where $a_0' = a_0/\log(R)$, $a_n' = a_nR^n$ and $b_n' = b_nR^n$. The third condition in (1.11) ensures that this is indeed the unique solution. Without this condition, any solution of the

Let us first look for a solution in the form a single layer potential, as defined by (1.2). Then everything works just like in Section 1.1: For $\boldsymbol{x} \in \Gamma$, the limiting value of $u(\boldsymbol{x}')$ as $\boldsymbol{x}' \to \boldsymbol{x}$ for $\boldsymbol{x}' \in \Omega$ satisfies the simple relation (1.5), and so the BIE formulation of (1.11) is again

$$\int_\Gamma \phi(\boldsymbol{x}-\boldsymbol{y})\,\sigma(\boldsymbol{y})\,ds(\boldsymbol{y}) = f(\boldsymbol{x}), \qquad \boldsymbol{x} \in \Gamma. \tag{1.12}$$

The formulation (1.12) has two advantages over (1.11): First, it represents an equation on a *bounded* domain, which makes discretization easy. Second, by using an integral representation like (1.2), we satisfy the decay condition at infinity *automatically*; no additional work is necessary. However, the simple single layer formulation (1.12) results upon discretization in linear systems that are not particularly well-conditioned.

To find a well-conditioned BIE formulation for (1.11), we might be tempted to look for a solution that is represented by a double layer potential, as in (1.6). But this will not in general work since one can easily see that while a solution of (1.11) may grow logarithmically as $\boldsymbol{x} \to \infty$, any solution of the form (1.6) will decay as $O(|\boldsymbol{x}|^{-1})$. To include a term with logarithmic growth, we enrich the set of solutions by adding the field from a point source inside the contour Γ, so that

$$u(\boldsymbol{x}) = \int_\Gamma d(\boldsymbol{x},\boldsymbol{y})\,\sigma(\boldsymbol{y})\,ds(\boldsymbol{y}) - \frac{1}{2\pi}\log|\boldsymbol{x}-\boldsymbol{z}| \int_\Gamma \sigma(\boldsymbol{y})\,ds(\boldsymbol{y}), \qquad \boldsymbol{x} \in \Omega, \tag{1.13}$$

where $\boldsymbol{z}$ is a fixed point that we pick in the *interior* of Γ. This formulation leads to the well-posed Fredholm equation of the second kind

$$\frac{1}{2}\sigma(\boldsymbol{x}) + \int_\Gamma \left(d(\boldsymbol{x},\boldsymbol{y}) - \frac{1}{2\pi}\log|\boldsymbol{x}-\boldsymbol{z}| \right) \sigma(\boldsymbol{y})\,ds(\boldsymbol{y}) = f(\boldsymbol{x}), \qquad \boldsymbol{x} \in \Gamma. \tag{1.14}$$

Let us observe that the BIE formulation has allowed us to rewrite the problem (1.11) which was defined on the infinite domain Ω as the equation (1.14) that is defined on a finite domain. Moreover, the solution to (1.14) satisfies the decay conditions at infinity automatically.

1.4. The Helmholtz equation

Let us next consider a BVP involving the Helmholtz operator $-\Delta - \kappa^2 I$, where the wave number κ is a positive real number. To be precise, let Ω be a finite simply connected domain with a smooth boundary Γ. Then given a function f, we consider the Dirichlet problem

$$\begin{cases} -\Delta u(\boldsymbol{x}) - \kappa^2 u(\boldsymbol{x}) = 0, & \boldsymbol{x} \in \Omega, \\ u(\boldsymbol{x}) = f(\boldsymbol{x}), & \boldsymbol{x} \in \Gamma. \end{cases} \tag{1.15}$$

We recall that the fundamental solution of the Helmholtz operator is given by

$$\phi_\kappa(\boldsymbol{x}) = \frac{i}{4} H_0^{(1)}(\kappa|\boldsymbol{x}|),$$

where $H_0^{(1)}$ is the zero'th order Hankel function of the first kind. We then define the single and double layer kernels

$$s_\kappa(\boldsymbol{x},\boldsymbol{y}) = \phi_\kappa(\boldsymbol{x}-\boldsymbol{y}), \qquad \text{and} \qquad d_\kappa(\boldsymbol{x},\boldsymbol{y}) = \boldsymbol{n}(\boldsymbol{y}) \cdot \nabla_{\boldsymbol{y}} \phi_\kappa(\boldsymbol{x}-\boldsymbol{y}),$$

and the corresponding operators

$$[S_\kappa \sigma](\boldsymbol{x}) = \int_\Gamma s_\kappa(\boldsymbol{x},\boldsymbol{y})\,\sigma(\boldsymbol{y})\,ds(\boldsymbol{y}), \qquad \text{and} \qquad [D_\kappa \sigma](\boldsymbol{x}) = \int_\Gamma d_\kappa(\boldsymbol{x},\boldsymbol{y})\,\sigma(\boldsymbol{y})\,ds(\boldsymbol{y}).$$

---

form $u(r,\theta) = a_0' \log(r) + a_0'' + \sum_{n=1}^\infty \left[\left(\frac{a_n'}{r^n} + a_n'' r^n \right) \cos(n\theta) + \left(\frac{b_n'}{r^n} + b_n'' r^n \right) \sin(n\theta) \right]$ would also satisfy $-\Delta u = 0$ and the Dirichlet condition as long as $a_n'/R^n + a_n'' R^N = a_n$ and $b_n'/R^N + b_n'' R^n = b_n$. In other words, with each Fourier mode, there are two independent solutions to the exterior problem, and the job of the decay condition at infinity is to ensure uniqueness in the solution by picking one of them.

The function ϕ_κ has the same singularity as ϕ at the origin,

$$\phi_\kappa(\boldsymbol{x}) = -\frac{1}{2\pi}\log|\boldsymbol{x}| + O(1), \qquad \text{as } \boldsymbol{x} \to \boldsymbol{0}.$$

This means that the double layer potential has the same limiting behavior as we approach the boundary

$$\lim_{\boldsymbol{x}'\to\boldsymbol{x},\boldsymbol{x}'\in\Omega} \int_\Gamma d_\kappa(\boldsymbol{x}',\boldsymbol{y})\,\sigma(\boldsymbol{y})\,ds(\boldsymbol{y}) = -\frac{1}{2}\sigma(\boldsymbol{x}) + \int_\Gamma d_\kappa(\boldsymbol{x},\boldsymbol{y})\,\sigma(\boldsymbol{y})\,ds(\boldsymbol{y}). \tag{1.16}$$

It might now be natural to look for a solution to (1.21) in the form

$$u(\boldsymbol{x}) = \int_\Gamma d_\kappa(\boldsymbol{x},\boldsymbol{y})\,\sigma(\boldsymbol{y})\,ds(\boldsymbol{y}), \qquad \boldsymbol{x}\in\Omega. \tag{1.17}$$

Using (1.16), we find that σ must satisfy

$$-\frac{1}{2}\sigma(\boldsymbol{x}) + [D_\kappa\sigma](\boldsymbol{x}) = f(\boldsymbol{x}), \qquad \boldsymbol{x}\in\Gamma, \tag{1.18}$$

which is a Fredholm equation of the second kind. However, there is a catch: There exist wave-numbers κ for which (1.15) is well-defined, but for which (1.18) is not. These are called "spurious" or "artificial" resonances. To obtain a BIE that is well-defined whenever the BVP is well-defined, we instead of (1.17) look for a solution that is a linear combination of a single layer and a double layer potential. The so called "combined field" formulation takes the form We look for a solution of the form

$$u(\boldsymbol{x}) = [(D_\kappa + i\eta S_\kappa)\sigma](\boldsymbol{x}) = \int_\Gamma \big(d_\kappa(\boldsymbol{x},\boldsymbol{y}) + i\eta s_\kappa(\boldsymbol{x},\boldsymbol{y})\big)\,\sigma(\boldsymbol{y})\,ds(\boldsymbol{y}), \tag{1.19}$$

where η is a parameter that is often chosen as $\eta = \pm\kappa$. The function σ is then determined by solving the second kind Fredholm equation

$$-\frac{1}{2}\sigma(\boldsymbol{x}) + \int_\Gamma \big(d_\kappa(\boldsymbol{x},\boldsymbol{y}) + i\eta s_\kappa(\boldsymbol{x},\boldsymbol{y})\big)\,\sigma(\boldsymbol{y})\,ds(\boldsymbol{y}) = f(\boldsymbol{x}), \qquad \boldsymbol{x}\in\Gamma. \tag{1.20}$$

The BIE (1.20) is now a Fredholm equation of the second kind that is well-posed for every κ for which (1.21) is well-posed.

1.5. Radiation conditions for the Helmholtz equation

Our final example of rewriting a PDE as a BIE is a Helmholtz equation on an exterior domain that models, e.g., time harmonic wave problems. This is a showcase example for the usefulness of BIE formulations. To be specific, we will consider the so called "sound soft" acoustic scattering problem modeled by the equation

$$\begin{cases} -\Delta u(\boldsymbol{x}) - \kappa^2 u(\boldsymbol{x}) = 0, & \boldsymbol{x}\in\Omega, \\ u(\boldsymbol{x}) = f(\boldsymbol{x}), & \boldsymbol{x}\in\Gamma, \\ \lim_{r\to\infty}\sqrt{r}\left(\dfrac{\partial u(r\boldsymbol{z})}{\partial r} - i\kappa u(r\boldsymbol{z})\right) = 0, & \text{for every unit vector } \boldsymbol{z}, \end{cases} \tag{1.21}$$

where the wave number κ is a real positive number, and where Ω is a domain exterior to a smooth contour Γ, as shown in Figure ?.

Following the treatment in Section 1.4, we look for a solution in the form of a combined field

$$u(\boldsymbol{x}) = [(D_\kappa + i\eta S_\kappa)\sigma](\boldsymbol{x}) = \int_\Gamma \big(d_\kappa(\boldsymbol{x},\boldsymbol{y}) + i\eta s_\kappa(\boldsymbol{x},\boldsymbol{y})\big)\,\sigma(\boldsymbol{y})\,ds(\boldsymbol{y}). \tag{1.22}$$

The function σ is determined by solving the second kind Fredholm equation

$$\frac{1}{2}\sigma(\boldsymbol{x}) + \int_\Gamma \big(d_\kappa(\boldsymbol{x},\boldsymbol{y}) + i\eta s_\kappa(\boldsymbol{x},\boldsymbol{y})\big)\,\sigma(\boldsymbol{y})\,ds(\boldsymbol{y}) = f(\boldsymbol{x}), \qquad \boldsymbol{x}\in\Gamma. \tag{1.23}$$

The formula (1.22) has the advantage that the resulting BIE (1.20) is a Fredholm equation of the second kind; it is well-posed for every κ; it is defined on a finite domain; and the radiation condition at infinity is satisfied automatically.

Let us stress that solving the (1.21) by directly discretizing the PDE would be quite challenging. In practical application, it is not uncommon to artificially truncate the infinite exterior domain, and to apply some boundary condition that to some degree of accuracy mimics the effect of the "radiation condition" at infinity. It is not easy to do this without substantial loss of accuracy, however, which makes the ability to reformulate the problem as a BIE particularly valuable.

1.6. Summary and discussion

We have seen in this chapter that when a good integral equation formulation for a physical problem is available, then this often provides an excellent starting point for numerical simulations. Benefits include:

(1) The condition number of the linear system that arises is typically similar to the condition number of the actual "physics" of the problem. This is in contrast to discrete systems arising from discretizations of differential equations, which typically have very large condition numbers. (High condition numbers lead to several difficulties; loss of accuracy being one.)

(2) The computational complexity is asymptotically optimal in the sense that it scales linearly with what is arguably the actual *inherent* complexity of the problem. This effect is most obvious for a problem in which data is prescribed only on the boundary of the domain, such as in (1.1), since in this case, the BIE is itself defined only on the boundary, and the number of discretization nodes required depends only on the complexity of Γ, and on the regularity of the boundary data f. (Since the given data is defined on a set of dimension $d-1$ we should not have to discretize a set of dimension d!)

(3) Handling *exterior* problems where the domain Ω is the region outside some given contour or surface Γ is quite hard when discretizing the differential equation. Typically some artificial external boundary is introduced. In contrast, when using a BIE, the equation is inherently formulated on the finite domain Γ, and no such difficulties arise.

Despite the advantages of integral equation formulations, there are many situations where discretizing the PDE remains a better course of action. For problems involving variable coefficient differential operators, and/or body loads that act on the interior of the domain Ω, the integral equation formulation loses some of its most obvious advantages. (The gain in conditioning remains a powerful advantage, though, cf. Sections 3.3 and 3.4.) There are also more prosaic reasons for sometimes preferring methods based on PDE formulations in that such methods are far better established, with a wealth of user friendly software available. For problems in 3D, having access to sophisticated machinery for handling geometric information, for performing automatic mesh refinement, etc., is often a deciding factor for a user

For future reference, let us write down a generic boundary integral equation defined on the boundary Γ of a domain Ω,

$$\alpha\sigma(\boldsymbol{x}) + \int_\Gamma k(\boldsymbol{x},\boldsymbol{y})\,\sigma(\boldsymbol{y})\,ds(\boldsymbol{y}) = f(\boldsymbol{x}), \qquad \boldsymbol{x}\in\Gamma. \tag{1.24}$$

In (1.24), the boundary Γ may be either a curve in $\mathbb{R}^2$ or a surface in $\mathbb{R}^3$. The "kernel function" $k(\boldsymbol{x},\boldsymbol{y})$ is typically (but not always) singular as $|\boldsymbol{x}-\boldsymbol{y}|\to 0$. In this text, almost all integral operators involve kernels whose singularities are sufficiently mild that the integral is well defined in a standard sense as a Lebesgue integral or as a generalized Riemann integral; we call such an integral operator "weakly singular". Let us

note that it is in practice quite common to work with integral operators with more strongly singular kernels, in which case the operator must be interpreted a principal value in some sense. Before closing this chapter, let us again remember that for any given boundary value problem, there are often a slew of different ways to formulate it as a BIE, and that choosing the right BIE that leads to a benign mathematical formulation is an important part of the process.

CHAPTER 2

Discretization of Integral Equations

In Chapter 1, we described how a boundary value problem (BVP) defined on a domain Ω can in many situations be rewritten as a boundary integral equations (BIE) defined only on the boundary Γ of Ω. For instance, we showed that the BVP

$$\begin{cases} -\Delta u(\boldsymbol{x}) = 0 & \text{for } \boldsymbol{x} \in \Omega, \\ u(\boldsymbol{x}) = f(\boldsymbol{x}) & \text{for } \boldsymbol{x} \in \Gamma, \end{cases} \tag{2.1}$$

could alternatively be formulated as the BIE

$$\int_\Gamma k(\boldsymbol{x}, \boldsymbol{y})\, \sigma(\boldsymbol{y})\, ds(\boldsymbol{y}) = f(\boldsymbol{x}), \qquad \boldsymbol{x} \in \Gamma, \tag{2.2}$$

where

$$k(\boldsymbol{x}, \boldsymbol{y}) = -\frac{1}{2\pi} \log |\boldsymbol{x} - \boldsymbol{y}|.$$

In this chapter, we will describe how to take the next step of converting an equation such as (2.2) into a discrete equation

$$\mathbf{A}\boldsymbol{\sigma} = \mathbf{f},$$

whose solution $\boldsymbol{\sigma}$ represents an approximate solution to (2.2). The central task we need to resolve is how to numerically evaluate an integral such as

$$u(\boldsymbol{x}) = \int_\Gamma k(\boldsymbol{x}, \boldsymbol{y})\, \sigma(\boldsymbol{y})\, ds(\boldsymbol{y}), \tag{2.3}$$

where k is one of the kernels that arise in rewriting an elliptic PDE, and $\boldsymbol{x}$ is a point on the boundary Γ. The difficulty we encounter is that most of the kernel functions $k(\boldsymbol{x}, \boldsymbol{y})$ that we need to work with have singularities as $\boldsymbol{y} \to \boldsymbol{x}$. Finding techniques that simultaneously are simple to use, lead to high accuracy, and are computationally efficient, turns out to be more challenging than one might have hoped. The search for such methods remains an active area of research, in particular for 3D problems where Γ is a surface.

Our objective in this chapter is to provide a gentle introduction to the key concepts. We will describe in some detail methods that are conceptually simple and easy to implement. These methods can be extremely accurate for BIEs that happen to have smooth kernels. However, for a more typical BIE, they obtain only convergence of order $O(h)$ or less as the mesh refinement parameter $h \to 0$. There are ways to fix this to obtain methods with convergence order $O(h^p)$ for very large p (say $p = 10$ or $p = 20$), even for singular kernels. These techniques are more complex, and we will limit ourselves to providing a high-level description of how they work, and how they are used; and then provide references to the literature for more details.

REMARK 2.1 (Collocation methods versus boundary element methods). *An important question to consider when developing numerical methods for solving an equation involving a function of a continuum variable is how best to represent the function in a computationally convenient manner. In different words, an equation such as (2.2) is most naturally viewed as being defined in an infinite dimensional vector space such as $V = L^2(\Gamma)$. For computational work, we must restrict the equation to some finite dimensional subspace $V_N \subset V$. A common approach here is to introduce a set of basis functions $\{\varphi_j\}_{j=1}^N$, and then let a vector $\boldsymbol{\sigma} \in \mathbb{R}^N$ represent the function $\sigma(\boldsymbol{x}) = \sum_{j=1}^N \boldsymbol{\sigma}(j)\, \varphi_j(\boldsymbol{x})$. In contrast, we will in this text focus on techniques where a function is represented simply via a vector $\boldsymbol{\sigma}$ of pointwise values $\boldsymbol{\sigma}(j) = \sigma(\boldsymbol{x}_j)$, where*

$\{\boldsymbol{x}_j\}_{j=1}^N$ is a fixed set of so called collocation nodes. Each set of techniques come with advantages and disadvantages. Methods based on basis expansions tend to be easier to use for purposes of mathematical analysis, while collocation methods can be easier to use in practice.

2.1. Parameterization of curves

In order to evaluate an integral such as (2.3), it is convenient to first parameterize the contour Γ to convert it to a standard scalar integral. Let us for simplicity restrict attention to some simple contour Γ that can be parameterized using a piecewise smooth periodic function

$$\boldsymbol{G}:\ I \to \mathbb{R}^2, \tag{2.4}$$

where I is an interval. In other words, $\Gamma = \{\boldsymbol{G}(t):\ t \in I\}$. Then the integral (2.3) can be written as

$$u(\boldsymbol{x}) = \int_I k(\boldsymbol{x}, \boldsymbol{G}(t))\, \sigma(\boldsymbol{G}(t))\, |\boldsymbol{G}'(t)|\, dt. \tag{2.5}$$

Before we move to the discussion on how to numerically evaluate the scalar integral (2.5), it is perhaps helpful to spend a few moments describing the behavior of the function

$$\varphi(t) = k(\boldsymbol{x}, \boldsymbol{G}(t))\, |\boldsymbol{G}'(t)|$$

for some representative geometries. To be precise, we will consider the four geometries shown in the left column of Figure 2.1. For each geometry, we plot in the right column the function φ for two kernel functions:

$$\begin{aligned} &\textit{The single layer potential:} \quad k(\boldsymbol{x}, \boldsymbol{y}) = -\frac{1}{2\pi} \log|\boldsymbol{x} - \boldsymbol{y}|, \\ &\textit{The double layer potential:} \quad k(\boldsymbol{x}, \boldsymbol{y}) = \frac{(\boldsymbol{x} - \boldsymbol{y}) \cdot \boldsymbol{n}(\boldsymbol{y})}{2\pi |\boldsymbol{x} - \boldsymbol{y}|^2}. \end{aligned}$$

In the top row, the contour is simply the ellipse defined by $\boldsymbol{G}(t) = (1.3\cos(t),\ 0.6\sin(t))$ where $t \in [-\pi, \pi]$, and the target point $\boldsymbol{x} = (1, 0)$ is on the inside, well separated from the contour itself. In this case, the points $\boldsymbol{x}$ and $\boldsymbol{y} = \boldsymbol{G}(t)$ are never close to touching, and the function φ is a C^∞ periodic function for both kernels. The second row shows the same geometry, but with the target point $\boldsymbol{x}$ moved very close to the contour, with $\boldsymbol{x} = (1.28, 0)$. In this case the function φ is still C^∞, but has very sharp derivatives in the region where $\boldsymbol{G}(t)$ is close to $\boldsymbol{x}$. In the third row, we move the target point onto to contour, $\boldsymbol{x} = (1.3, 0)$. Now the double layer kernel is smooth, while the single layer kernel develops a logarithmic singularity. In the fourth row, we consider a piecewise smooth contour, and a target point $\boldsymbol{x}$ that sits on the contour itself. For the single layer kernel, φ has a logarithmic singularity when $\boldsymbol{G}(t) \to \boldsymbol{x}$, but is otherwise a continuous function. In contrast, for the double layer kernel, there is no singularity at the point where $\boldsymbol{G}(t) \to \boldsymbol{x}$, but on the other hand the function φ is discontinuous at the points where the normal $\boldsymbol{n}(t)$ is discontinuous.

REMARK 2.2. *In most cases, the kernel $k(\boldsymbol{x}, \boldsymbol{y})$ in a BIE is singular as $\boldsymbol{y} \to \boldsymbol{x}$, but recall that the double layer kernel*

$$d(\boldsymbol{x}, \boldsymbol{y}) = -\frac{\boldsymbol{n}(\boldsymbol{y}) \cdot (\boldsymbol{x} - \boldsymbol{y})}{2\pi |\boldsymbol{x} - \boldsymbol{y}|^2},$$

happens to be smooth when the contour is smooth. Using a parameter map such as (2.4), we can easily evaluate the limiting value at the diagonal. Using l'Hôpital's rule twice, we find that

$$\lim_{t' \to t} D(\boldsymbol{G}(t), \boldsymbol{G}(t')) = -\frac{G_2'(t)\, G_1''(t) - G_1'(t)\, G_2''(t)}{4\pi |G'(t)|^3}.$$

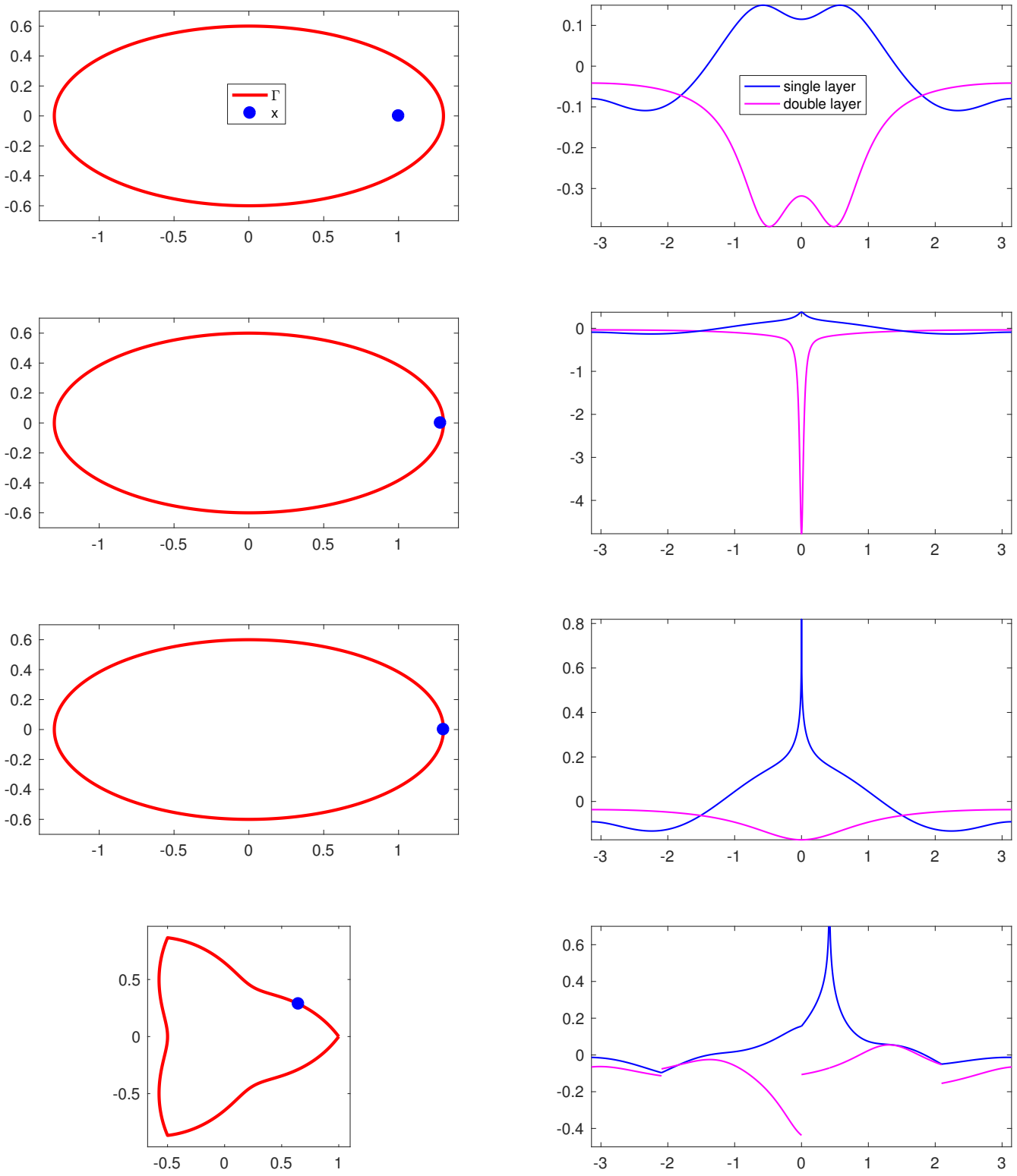

FIGURE 2.1. The pictures in the left column show four contours Γ, each with a target point $\boldsymbol{x}$ marked, cf. Section 2.1. For each geometry, the corresponding plot in the right column shows the function $\varphi(t) = k(\boldsymbol{x}, \boldsymbol{G}(t))\,|\boldsymbol{G}'(t)|$, where $\boldsymbol{G}$ is a function such that $\Gamma = \{\boldsymbol{G}(t) : t \in [-\pi, \pi]\}$. (To be precise, $\boldsymbol{G}(t) = (r(t)\cos(t),\, r(t)\sin(t))$ for some function $r(t)$.) The blue/magenta lines show the single/double layer kernels, respectively.

2.2. The Trapezoidal rule

The first numerical method that we describe for evaluating the integral in (2.3) uses a set of quadrature nodes that is equispaced in the parameter domain. This rule is very simple to use, and is best suited for smooth contours. Despite its simplicity, this method can give exceptionally high accuracy when the integrand in the parameterized integral (2.5) is smooth, as happens when the target point $\boldsymbol{x}$ is not close to the contour Γ itself, as well as in the rare cases where the kernel function $k(\boldsymbol{x}, \boldsymbol{y})$ is smooth.

To be precise, let us suppose that Γ is a smooth contour that is parameterized via a periodic function

$$\boldsymbol{G}:\ [0,T] \rightarrow \mathbb{R}^2,$$

so that $\Gamma = \{\boldsymbol{G}(t):\ t \subset [0,T]\}$. This is precisely the framework introduced in Section 2.1, for the case when $I = [0,T]$. Given a positive integer N, we pick N equispaced nodes $\{t_i\}_{i=1}^N \in I$, where $t_i = ih$ for $h = 1/T$. We can then apply the Trapezoidal rule to the parameterized integral in (2.5) to obtain the approximation

$$u(\boldsymbol{x}) \approx h \sum_{i=1}^{N} k(\boldsymbol{x}, \boldsymbol{G}(t_i))\, \sigma(\boldsymbol{G}(t_i))\, |\boldsymbol{G}'(t_i)|. \tag{2.6}$$

Observe that since the integrand is periodic, all nodes have the same quadrature weight h. (In contrast to a non-periodic interval, in which case each of the two end-points would have weight $h/2$.) To simplify the formula (2.6), we set

$$\begin{aligned} \boldsymbol{x}_i &= \boldsymbol{G}(t_i), \\ w_i &= h\, |\boldsymbol{G}'(t_i)|, \end{aligned}$$

so that the approximation can be written

$$u(\boldsymbol{x}) \approx \sum_{i=1}^{N} k(\boldsymbol{x}, \boldsymbol{x}_i)\, \sigma(\boldsymbol{x}_i)\, w_i. \tag{2.7}$$

We note that if the parameter t is arc-length, then of course $|\boldsymbol{G}'(t)| = 1$ for every t, so $w_i = h$.

When the target point $\boldsymbol{x}$ does not lie on Γ, the integrand in (2.5) is a C^∞ periodic function on $[0,T]$. (Recall that we assumed that the contour is smooth in this section.) It is known that for such a function, the Trapezoidal rule is remarkably accurate; it results in an error that goes to zero faster than N^{-p} for any positive integer p.

When $\boldsymbol{x} \in \Gamma$, the situation becomes more complicated. For a kernel with a weakly integrable singularity, the approximation in (2.7) converges to zero as $h \rightarrow$, but very slowly. For instance, for a kernel with a logarithmic singularity, such as the single layer potential, convergence is typically of the order $O(h \log(1/h))$.

The remarkable fact that the double layer kernel is in fact smooth when $\boldsymbol{x} \in \Gamma$ means that the Trapezoidal rule converges super-polynomially fast for this particular case, even when $\boldsymbol{x} \in \Gamma$.

REMARK 2.3 (Near curve evaluation). *A situation that is mathematically benign, but that has led to many headaches in practice arises when the target point $\boldsymbol{x}$ lies close to the contour, as shown on the second row in Figure 2.1. Let $d = \inf\{|\boldsymbol{x} - \boldsymbol{y}|:\ \boldsymbol{y} \in \Gamma\}$ denote the distance between $\boldsymbol{x}$ and Γ. As long as $d > 0$, the integrand in (2.3) is C^∞. However, if d is comparable to the discretization resolution h, then the derivatives of the function $t \mapsto k(\boldsymbol{x}, \boldsymbol{G}(t))\, \sigma(\boldsymbol{G}(t))\, |\boldsymbol{G}'(t)|$ get so large that one typically loses all accuracy in the quadrature. Specialized techniques have been developed for this case, as described in, e.g., [??].*

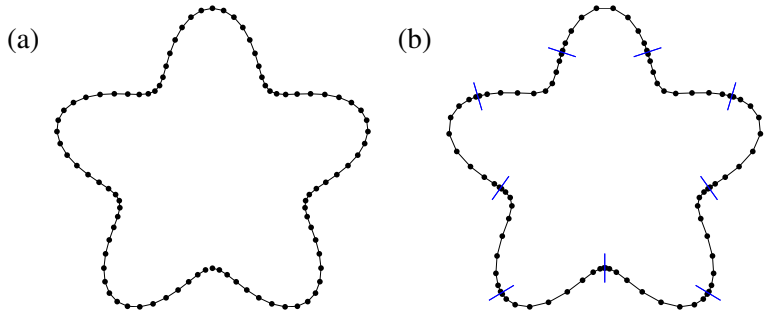

FIGURE 2.2. Example of a smooth planar curve discretized with $N = 90$ points via (a) periodic trapezoid rule nodes and (b) panel-based rule (10-point Gauss–Legendre; the panel ends are shown by line segments). In both cases the parametrization is polar angle $t \in [0, 2\pi]$ and the curve is the radial function $f(t) = 9/20 - (1/9)\cos(5t)$.

2.3. Panel based quadrature rules

While the Trapezoidal rule often works very well for closed smooth contours, it is not always easy to find a global parameter function $\boldsymbol{G}$. Moreover, even when such a function can be found, it is not always desirable to have the distribution of quadrature points restricted by a requirement that they be equispaced in the parameter domain. There are often certin areas on the contour where the integrand changes rapidly, and where we want to put points more densely. Areas where the curvature is high, or where the contour comes close to touching itself or another contour would be typical examples. Moreover, for a contour that is only piecewise smooth, any global rule such as the Trapezoidal rule would lose accuracy dramatically. In situations like these, so called "panel-based" quadratures are generally preferred. The idea is to split the contour Γ into disjoint pieces

$$\Gamma = \Gamma_1 \cup \Gamma_2 \cup \cdots \cup \Gamma_m,$$

and then evaluate the integral over each piece Γ_j separately. To this end, let us for each Γ_j introduce a local parameter map

$$\boldsymbol{G}_j : [0, 1] \to \Gamma_j.$$

We can then write

$$u(\boldsymbol{x}) = \sum_{j=1}^{m} \int_{\Gamma_j} k(\boldsymbol{x}, \boldsymbol{y})\, \sigma(\boldsymbol{y})\, ds(\boldsymbol{y}) = \sum_{j=1}^{m} \int_0^1 k(\boldsymbol{x}, \boldsymbol{G}_j(t))\, \sigma(\boldsymbol{G}_j(t))\, |\boldsymbol{G}_j'(t)|\, dt.$$

When the target point $\boldsymbol{x}$ is placed away from the contour, each of the integrals involves a smooth integrand, and we can use, e.g., Gauss-Legendre quadrature to evaluate them to high accuracy. If we place p Legendre nodes on $[0, 1]$, then the resulting quadrature involves $N = mp$ total points $\{\boldsymbol{x}_i\}_{i=1}^N$, and again leads to a formula of the form

$$u(\boldsymbol{x}) \approx \sum_{i=1}^{N} k(\boldsymbol{x}, \boldsymbol{x}_i)\, \sigma(\boldsymbol{x}_i)\, w_i.$$

The quadrature error goes to zero as $(1/m)^{2p-1}$ as $m \to \infty$ in this case. Panel based quadratures of this type often lead to very high accuracy, and offer more flexibility than a global quadrature such as the Trapezoidal rule.

For the case where the kernel function is smooth, we retain the same high convergence speed even when $\boldsymbol{x} \in \Gamma$. However, in the more typical case of singular integrals, correction techniques such as those described in Section 2.8 will be required.

2.4. Nyström discretization

Suppose we a given an integral equation of a continuum variable such as

$$b\sigma(\boldsymbol{x}) + \int_\Gamma k(\boldsymbol{x},\boldsymbol{y})\,\sigma(\boldsymbol{y})\,ds(\boldsymbol{y}) = f(\boldsymbol{x}), \qquad \boldsymbol{x}\in\Gamma \tag{2.8}$$

and seek to compute an approximate solution. The first step is to find a way to "discretize" the equation, to convert it into a linear system $\mathbf{A}\boldsymbol{\sigma} = \mathbf{f}$, where $\mathbf{A}$ is an $N\times N$ matrix. To do this using the Nyström technique, we start with an underlying quadrature scheme on the domain Γ, defined by nodes $\{\boldsymbol{x}_i\}_{i=1}^N \subset \Gamma$, and corresponding weights $\{w_i\}_{i=1}^N$. We typically use a rule such that for a smooth function g that is defined on Γ, it is that case that

$$\int_\Gamma g(\boldsymbol{x})ds(\boldsymbol{x}) \approx \sum_{i=1}^N w_i g(\boldsymbol{x}_i) \tag{2.9}$$

holds to high accuracy. Here, one could use a panel based quadrature, as described in Section 2.3, or, for the case of a smooth contour, the Trapezoidal rule described in Section 2.2. The Nyström method for discretizing (2.8) then constructs a linear system that relates a given data vector $\mathbf{f} = \{f_i\}_{i=1}^N$ where $f_i = f(\boldsymbol{x}_i)$ to an unknown solution vector $\boldsymbol{\sigma} = \{\sigma_i\}_{i=1}^N$ where $\sigma_i \approx \sigma(\boldsymbol{x}_i)$. Informally speaking, the idea is to use the nodes $\{\boldsymbol{x}_i\}_{i=1}^N$ as *collocation points* where (2.8) is enforced:

$$b\sigma(\boldsymbol{x}_i) + \int_\Gamma k(\boldsymbol{x}_i,\boldsymbol{y})\sigma(\boldsymbol{y})\,ds(\boldsymbol{y}) = f(\boldsymbol{x}_i), \qquad i = 1,\,2,\,\ldots,N. \tag{2.10}$$

Then matrix elements $\{\mathbf{A}(i,j)\}_{i,j=1}^N$ are constructed such that, for a smooth function σ on Γ,

$$\int_\Gamma k(\boldsymbol{x}_i,\boldsymbol{y})\sigma(\boldsymbol{y})\,ds(\boldsymbol{y}) \approx \sum_{j=1}^N \mathbf{A}(i,j)\,\sigma(\boldsymbol{x}_j). \tag{2.11}$$

Combining (2.10) and (2.11) we obtain a square linear system that relates $\boldsymbol{\sigma}$ to $\mathbf{f}$:

$$b\sigma_i + \sum_{j=1}^N \mathbf{A}(i,j)\,\sigma_j = f_i, \qquad i = 1,\,2,\,\ldots,\,N. \tag{2.12}$$

We write (2.12) in matrix form as

$$b\boldsymbol{\sigma} + \mathbf{A}\boldsymbol{\sigma} = \mathbf{f}. \tag{2.13}$$

Once $\boldsymbol{\sigma}$ has been found, an approximation to $\sigma(\boldsymbol{x})$ for general $\boldsymbol{x}\in\Gamma$ may then be constructed by interpolation through the values provided in the vector $\boldsymbol{\sigma}$.

Let us first consider a case where the kernel function k is smooth, as happens for the double layer operator associated with the Laplace equation in two dimensions (1.10). In this case, we can simply choose the matrix elements in $\mathbf{A}$ via the formula

$$\mathbf{A}(i,j) = k(\boldsymbol{x}_i,\boldsymbol{x}_j)\,w_j. \tag{2.14}$$

This leads to an error convergence rate that is provably of the same order as the underlying quadrature scheme [**7**, Sec. 12.2].

Unfortunately, it is rare that we are lucky enough that a BIE has a smooth kernel. It is more typical for the kernel to have a singularity, in which case specialized quadrature rules that are designed specifically for singular kernels must be employed if high order accuracy is to be attained. We provide brief a brief introduction to these techniques in Sections 2.7 and 2.8.

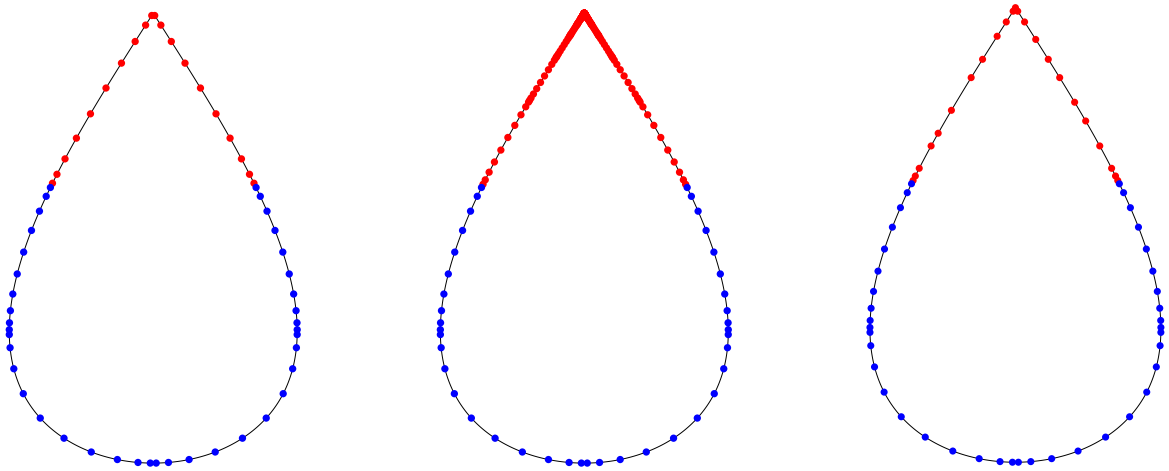

(a) (b) (c)

FIGURE 2.3. A contour Γ with a corner. (a) The original Gaussian grid before refinement, red nodes in Γ_1 and blue in Γ_2. (b) The locally refined grid. (c) The grid after local compression.

2.5. Domains with corners

So far in this chapter, we have generally assumed that the contour Γ is smooth. Now let us consider a BIE such as (2.8) defined on a contour that is only piece-wise smooth, with the pieces joined together to form corners. A very simple example with a single corner is shown in Figure 2.3(a). Now in addition to the fact that the kernel function $k(\boldsymbol{x}, \boldsymbol{y})$ is typically singular as $\boldsymbol{y} \rightarrow \boldsymbol{x}$, an additional difficulty arises in that the function σ that solves (2.8) also lacks regularity at the corner.

To describe the refinement and the local compression, we consider a contour with a single corner, like the one in Figure 2.3(a). We partition the contour into two disjoint parts, $\Gamma = \Gamma_1 \cup \Gamma_2$, in such a way that Γ_1 is a small piece containing the corner. The piece Γ_2 is smooth, and can be discretized into panels rather coarsely (since we use a high order rule, high accuracy does not require many points). For the piece Γ_1, we use a simplistic refinement strategy where we recursively cut the panel nearest the corner in half. Once the innermost panel is small enough that its contribution can be ignored (recall that we assume that the integrand is integrable), we can stop the refinement.

As an alternative to simply refining around a corner singularity, one may exploit analytic knowledge of the exact form of the singularity that develop. This could be done by enriching the local space of approximating functions, or by developing specialized quadrature rules that can to high accuracy evaluate the action of the integral operator when applied to a layer potential with the relevant singularity. We refer to **[5, 2, 9, 3]** and the references therein for additional details.

2.6. Weighted norms

A reasonable critique of the Nyström discretization method is that the selection of nodes is driven purely by the objective of accurately evaluating an integral, with no regard to whether they actually form optimal collocation nodes. This concern becomes particularly relevant in situations where a large number of nodes are clustered for purposes of resolving a singularity, say near a corner (as illustrated in Figure 2.3(b)). In such a situation, it also becomes less clear to what extent one should expect the discrete system to be well conditioned just because the continuum integral equation is well conditioned. In order to ameliorate concerns such as these, it is often convenient to scale the entries in the vectors that we use by the quadrature weights.

To provide more details, let us return to the situation discussed in Section 2.4: We want to solve the BIE (2.8), and have at our disposal quadrature nodes $\{\boldsymbol{x}_i\}_{i=1}^N$ and weights $\{w_i\}_{i=1}^N$ such that (2.9) holds. We then associate a given function g defined on Γ with the vector $\mathbf{g} \in \mathbb{R}^N$ defined by

$$\mathbf{g}(i) = w_i^{1/2}\, g(\boldsymbol{x}_i).$$

Then

$$\|\mathbf{g}\|_{\ell^2}^2 = \sum_{i=1}^N w_i |\mathbf{g}(\boldsymbol{x}_i)|^2 \approx \int_\Gamma |g(\boldsymbol{y})|^2\, ds(\boldsymbol{y}) = \|g\|_{L^2(\Gamma)}^2.$$

By analogously weighing the entries of the matrix $\mathbf{A}$ discretizing the integral operator in (2.8), then the matrix will be a much more faithful approximation to the integral operator, in the sense that as the quadrature errors converge to zero, then for instance the spectral norm of the matrix will converge to the norm of the operator as a function on $L^2(\Gamma)$. We can easily illustrate the principle for the case where k is a smooth kernel. In this case, the matrix entries would be

$$\mathbf{A}(i,j) = w_i^{1/2}\, k(\boldsymbol{x}_i, \boldsymbol{x}_j)\, w_j^{1/2}.$$

Then if $\mathbf{f} = \mathbf{A}\mathbf{g}$ and $f(\boldsymbol{x}) = \int_\Gamma k(\boldsymbol{x}, \boldsymbol{y}) g(\boldsymbol{y})\, ds(\boldsymbol{y})$, we would have

$$\|\mathbf{f}\|_{\ell^2}^2 = \sum_{i=1}^N w_i \left(\sum_{j=1}^N k(\boldsymbol{x}_i, \boldsymbol{x}_j) w_j^{1/2}\, w_j^{1/2} \mathbf{g}(\boldsymbol{x}_j) \right)^2 \approx \sum_{i=1}^N w_i \left(\int_\Gamma k(\boldsymbol{x}_i, \boldsymbol{y}) \mathbf{g}(\boldsymbol{y})\, ds(\boldsymbol{y}) \right)^2 \approx \|f\|_{L^2(\Gamma)}^2.$$

2.7. Modified Trapezoidal quadrature rules for singular kernels

In this section, we discuss techniques for accurately evaluating an integral operator

$$[K\sigma](\boldsymbol{x}) = \int_\Gamma k(\boldsymbol{x}, \boldsymbol{y}) \sigma(\boldsymbol{y})\, ds(\boldsymbol{y}), \qquad \boldsymbol{x} \in \Gamma, \tag{2.15}$$

involving a kernel $k(\boldsymbol{x}, \boldsymbol{y})$ that is singular as $|\boldsymbol{x} - \boldsymbol{y}| \to 0$. Our objective is not to provide a comprehensive overview of the subject, but merely to illustrate the kinds of ideas that can be brought to bear. In the interest of simplicity, we limit attention to the case of a smooth contour Γ in the plane, and a kernel with a logarithmic singularity, so that $k(\boldsymbol{x}, \boldsymbol{y}) = \log|\boldsymbol{x} - \boldsymbol{y}|\, a(\boldsymbol{x}, \boldsymbol{y}) + b(\boldsymbol{x}, \boldsymbol{y})$ for some smooth functions a and b. Moreover, we for now restrict attention to quadratures based on the trapezoidal rule described in Section 2.2. (We will discuss corrections to panel based quadratures in Section 2.8.) Following the notation introduced there, we consider a set of nodes $\{\boldsymbol{x}_j\}_{j=1}^N$ that are equispaced in the parameter domain $[0, T]$, so that $\boldsymbol{x}_j = G(t_j) = G(jh)$, where G is the parameter map, where $h = T/N$ is the grid spacing in parameter space, and where $t_j = jh$ are the nodes in parameter space.

In the setting under consideration, the essential task is to evaluate a 1D integral of the form

$$I(f) = \int_0^T f(t)\, dt, \tag{2.16}$$

where f is a function with a logarithmic singularity, so that

$$f(t) = \log\left(\sin\left(\frac{t\pi}{T} \right) \right) \varphi(t) + \psi(t), \qquad t \in (0, T), \tag{2.17}$$

for some smooth functions φ and ψ. Due to the periodicity of the problem, we only need to consider functions φ and ψ that are restrictions of smooth T-periodic functions. (This means that $\varphi(0) = \varphi(T)$, that $\varphi'(0) = \varphi'(T)$, and so on.) A simple method to solve this task would be to apply the basic Trapezoidal rule, using the formula

$$I_N^{\text{Trap}}(f) = \sum_{j=1}^{N-1} h f(t_j).$$

(Observe that with f as in (2.17), the values of $f(t_0)$ and $f(t_N)$ are not defined.) The error $|I_N^{\mathrm{Trap}}(f) - I(f)|$ can for a singular integrand not converge faster than $O(h)$, however. The idea of Kapur-Rokhlin quadrature [**6, 4**] is to add a small number of "correction weights" near the end-points, to try to boost the convergence order. Suppose for instance that we allow ourselves to modify a total of four weights, two on either side, so that

$$I_N^{\mathrm{KR}(2)} = \eta_1 h\big(f(t_1) + f(T_{N-1})\big) + \eta_2 h\big(f(t_2) + f(T_{N-2})\big) + \underbrace{\sum_{j=1}^{N-1} hf(t_j)}_{=I_N^{\mathrm{Trap}}(f)}.$$

Here we used that due to the symmetry of the problem, there are really only *two* free parameters rather than four, since the nodes within each pair $\{t_1, t_{N-1}\}$ and $\{t_2, t_{N-2}\}$ should be treated the same way. One can then show [**6**] that it is possible to choose η_1 and η_2 in such a way that

$$|I_N^{\mathrm{KR}(2)}(f) - I(f)| = O(h^2), \qquad \text{as } h \to 0.$$

The idea can be generalized to include more correction terms to attain higher orders. Generally, if m is a small integer, an m-point Kapur-Rokhlin rule takes the form

$$I_N^{\mathrm{KR}(m)} = \underbrace{\sum_{j=1}^{m} \eta_j h\big(f(t_j) + f(t_{n-j})\big)}_{\text{"correction terms"}} + \underbrace{\sum_{j=1}^{N-1} hf(t_j)}_{=I_N^{\mathrm{Trap}}(f)},$$

and attains accuracy

$$|I_N^{\mathrm{KR}(m)}(f) - I(f)| = O(h^m), \qquad \text{as } h \to 0.$$

One drawback of the Kapur-Rokhlin quadrature rule is that it is not as numerically stable as one could wish. In particular, the weights $\{\eta_j\}_{j=1}^m$ take on both positive and negative signs, and grow in magnitude quite substantially as m grows. In practice, it works very well for $m \leq 6$ or so, and then ill-conditioning gets progressively worse, and the rule should probably not be used for $m > 10$. A table of the weights for $m \in \{2, 6, 10\}$ is provided in Appendix A of [**4**].

Next let us consider what happens when we apply the Kapur-Rokhlin rule to an integral operator such as 2.15. Let us for simplicity consider the node $\boldsymbol{x}_N$ since then the singularity is placed at $t_N = T$ (or, equivalently, $t_N = 0$) in parameter space. We find

$$\begin{aligned}
[K\sigma](\boldsymbol{x}_N) &= \int_\Gamma k(\boldsymbol{x}_N, \boldsymbol{y})\sigma(\boldsymbol{y})\, ds(\boldsymbol{y}) \\
&\approx \underbrace{\sum_{j=1}^{m} \eta_j h\big(k(\boldsymbol{x}_N, G(t_j))|G'(t_j)|\sigma(\boldsymbol{x}_j) + k(\boldsymbol{x}_N, G(t_{N-j}))|G'(t_{N-j})|\sigma(\boldsymbol{x}_{N-j})\big)}_{\text{"correction terms"}} + \underbrace{\sum_{j=1}^{N-1} hk(\boldsymbol{x}_N, G(t_j))|G'(t_j)|}_{\text{Trapezoidal rule}}.
\end{aligned}$$

Next let us consider a node $\boldsymbol{x}_j$ corresponding to a parameter point t_j in the interior of the interval. The singularity is now placed at t_j rather than at $t = 0$, but a simple shift of the integration parameter (so that $t' = t - t_j$) will again result in an integral of the form (2.16) with an integrand of the form (2.17). The end result is simply a cyclic shift of the quadrature weights.

As a final step, let us assemble the $N \times N$ matrix $\mathbf{A}$ that is the coefficient matrix in a Nyström discretization when the Kapur-Rokhlin rule is used. The vast majority of the entries will take the simple form $\mathbf{A}(i,j) = hk(\boldsymbol{x}_i, \boldsymbol{x}_j)|G'(t_j)|$, as dictated by the formula (2.14) with the basic Trapezoidal rule weights $w_j = h|G'(t_j)|$. The effect of the correction terms will be to modify a small number of entries close to the diagonal, as shown in Figure 2.4(a) for the case $m = 2$. The diagonal entries themselves will be set to zero, and the m closest entries on either side of the diagonal will be modified. In Figure 2.4(a), the zero entries

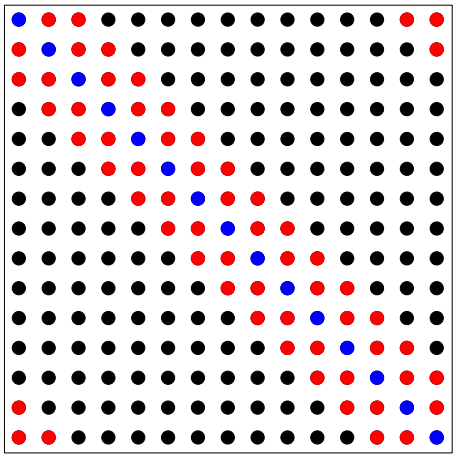

FIGURE 2.4. The pattern of a coefficient matrix $\mathbf{A}$ resulting from Nyström discretization of a BIE using the Kapur-Rokhlin quadrature, cf. Section 2.7 and formula (2.19). The figure shows the pattern of the matrix for the case where $N = 15$ and $m = 2$. The black entries follow the standard formula $\mathbf{A}(i,j) = k(\boldsymbol{x}_i, \boldsymbol{x}_j)w_j$. The red entries are modified by a multiplicative factor $(1 + \eta_\ell)$ so that $\mathbf{A}(i,j) = (1 + \eta_\ell)k(\boldsymbol{x}_i, \boldsymbol{x}_j)w_j$, where ℓ is the distance to the diagonal, cf. (2.18). The diagonal elements (blue) are all zero.

are blue, the modified entries are red, and the entries following the "regular" formula (2.14) are black. To give explicit formulas for the entries of $\mathbf{A}$, let us for indices $i, j \in \{1, 2, \ldots, N\}$ introduce a function $\ell(i,j)$ that measures "the distance to the diagonal" as follows:

$$\ell(i,j) = |\text{mod}(i - j, N)|, \tag{2.18}$$

where we use the convention that $\text{mod}(i, N)$ is an integer between $-N/2$ and $N/2$. To illustrate, for the case $N = 6$, the matrix $\mathbf{L}$ with entries $\mathbf{L}(i,j) = \ell(i,j)$ is simply

$$\mathbf{L} = \begin{bmatrix} 0 & 1 & 2 & 3 & 2 & 1 \\ 1 & 0 & 1 & 2 & 3 & 2 \\ 2 & 1 & 0 & 1 & 2 & 3 \\ 3 & 2 & 1 & 0 & 1 & 2 \\ 2 & 3 & 2 & 1 & 0 & 1 \\ 1 & 2 & 3 & 2 & 1 & 0 \end{bmatrix}.$$

With this distance function in hand, the formula for the coefficient matrix takes the form

$$\mathbf{A}(i,j) = \begin{cases} 0, & \text{when } i = j, \\ (1 + \eta_{\ell(i,j)})hk(\boldsymbol{x}_i, \boldsymbol{x}_j)|G'(t_j)|, & \text{when } \ell(i,j) \in \{1, 2, \ldots, m\}, \\ hk(\boldsymbol{x}_i, \boldsymbol{x}_j)|G'(t_j)|, & \text{when } \ell(i,j) > m. \end{cases} \tag{2.19}$$

To summarize, we have described a technique called "Kapur-Rokhlin quadrature" that is easy to use, and allows us to solve BIEs with logarithmically singular kernels to very high accuracy. The main drawback of Kapur-Rokhlin quadrature is that it is slightly numerically unstable, in particular for large m.

REMARK 2.4 (Alpert quadrature). *It turns out to be possible to build correction schemes to the Trapezoidal rule that attain the same $O(h^m)$ high order convergence, and are more numerically stable than the Kapur-Rokhlin rule. To illustrate, let us briefly outline the ideas underlying the so called "Alpert" quadrature rule, which leads to a coefficient matrix $\mathbf{A}$ where the vast number of entries are given by the standard formula $\mathbf{A}(i,j) = k(\boldsymbol{x}_i, \boldsymbol{x}_j)w_j$, with only a small number of entries close to the diagonal being modified, just like the Kapur-Rokhlin rule illustrated in Figure 2.4. The price to pay is that the derivation is more*

complex. Let us again consider the task of evaluating the integral (2.16) where f satisfies (2.17). We will now use a quadrature of the form

$$I_N^{\text{Alp}} = \underbrace{\sum_{j=1}^{m} \eta_j h\big(f(h\xi_j) + f(T - h\xi_j)\big)}_{\text{“correction terms”}} + \underbrace{\sum_{j=1}^{N-1} h f(t_j)}_{=I_N^{\text{Trap}}(f)}. \tag{2.20}$$

In (2.20), we have some new weights $\{\eta_j\}_{j=1}^m$, just as in the Kapur-Rokhlin rule. But we crucially also have some new nodes $\{\xi_j\}_{j=1}^m$. If we were to plug the rule (2.20) in directly to evaluate an integral such as (2.5), then we would find that it would involve evaluations of the function σ at points that are not among the collocation nodes $\{\boldsymbol{x}_j\}_{j=1}^N$. The trick here is to observe that while k has a singularity, the function σ is globally smooth. This means that $\sigma(\boldsymbol{x})$ can easily be expressed to high accuracy via local interpolation from some of the nearby equi-spaced nodes. For details on these constructions, we refer the reader to the original paper [**1**]*, and to the review article* [**4**].

2.8. Modified panel based quadrature rules for singular kernel

393C students: The text from this point onwards is still rough as of April 2. A more polished version should be posted within a week or so.

Let us consider the problem of how to discretize a BIE (1.24) when the kernel is weakly singular, and our “baseline” quadrature is panel based, rather than a global quadrature. For easy reference, let us restate a basic BIE

$$\alpha\sigma(\boldsymbol{x}) + \int_\Gamma k(\boldsymbol{x},\boldsymbol{y})\,\sigma(\boldsymbol{y})\,ds(\boldsymbol{y}) = f(\boldsymbol{x}), \qquad \boldsymbol{x}\in\Gamma, \tag{2.21}$$

where Γ is a smooth curve in the plane, where $k(\boldsymbol{x},\boldsymbol{y})$ is smooth for $\boldsymbol{x}\neq\boldsymbol{y}$, and $k(\boldsymbol{x},\boldsymbol{y}) \sim \log|\boldsymbol{x}-\boldsymbol{y}|$ as $\boldsymbol{y}\to\boldsymbol{x}$. We again start with a quadrature rule $\{\boldsymbol{x}_i, w_i\}_{i=1}^N$ designed for smooth functions

$$\int_\Gamma \varphi(\boldsymbol{y})\,dS(\boldsymbol{y}) \approx \sum_{i=1}^N w_i\,\varphi(\boldsymbol{x}_i), \qquad \text{for } \varphi \text{ smooth.}$$

In this section, we assume that this quadrature rule is a “panel based” Gauss-Legendre rule with p points within each panel, and a total of m panels so that $N = mb$, cf. Figure 2.5. Collocating at the quadrature nodes, we get the equation

$$\alpha\,\sigma(\boldsymbol{x}_i) + \int_\Gamma k(\boldsymbol{x}_i,\boldsymbol{y})\,\sigma(\boldsymbol{y})\,dS(\boldsymbol{y}) = f(\boldsymbol{x}_i), \qquad i = 1,\,2,\,3,\,\ldots,\,N.$$

Our task is now to construct an $N\times N$ matrix $\mathbf{A}$ such that

$$\sum_{j=1}^N \mathbf{A}(i,j)\,\sigma(\boldsymbol{x}_j) \approx \int_\Gamma k(\boldsymbol{x}_i,\boldsymbol{y})\,\sigma(\boldsymbol{y})\,dS(\boldsymbol{y}), \qquad i = 1,\,2,\,3,\,\ldots,\,N.$$

In what follows, it is important for us to remember the following: *The function σ that solves (2.21) is smooth, even though k is not.*

Let us fix an index i, and consider how to build the row $\mathbf{A}(i,:)$. This row seeks to evaluate the integral operator at the point $\boldsymbol{x} = \boldsymbol{x}_i$ as shown in Figure 2.5. We split the contour into three parts

$$\Gamma = \Gamma_{\text{self}} \cup \Gamma_{\text{near}} \cup \Gamma_{\text{far}},$$

where Γ_{self} is the panel that contains $\boldsymbol{x}_i$, Γ_{near} holds the two panels adjacent to Γ_{self}, and Γ_{far} holds all the other panels, cf. Figure 2.5. (For a more complicated contour, there may be other panels that happen to be

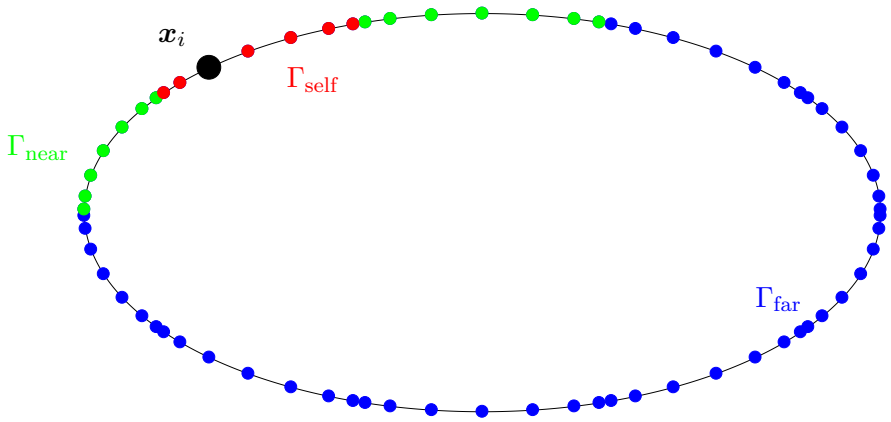

FIGURE 2.5. A contour Γ on which we seek to evaluating a boundary integral operator with a weakly singular kernel using a panel based quadrature, cf. Section 2.8. We consider a point $\boldsymbol{x}_i$ that is contained in a panel Γ_{self}. Panels immediately neighboring Γ_{self} form Γ_{near} and the remaining panels make up Γ_{far}.

located very close to Γ_{self} even though they may be far apart in parameter space. Such panels should then be included in Γ_{near}.) Then

$$\int_{\Gamma} k(\boldsymbol{x}_i, \boldsymbol{y})\, \sigma(\boldsymbol{y})\, dS(\boldsymbol{y}) = \int_{\Gamma_{\text{self}}} k(\boldsymbol{x}_i, \boldsymbol{y})\, \sigma(\boldsymbol{y})\, dS(\boldsymbol{y}) + \int_{\Gamma_{\text{near}}} k(\boldsymbol{x}_i, \boldsymbol{y})\, \sigma(\boldsymbol{y})\, dS(\boldsymbol{y}) + \int_{\Gamma_{\text{far}}} k(\boldsymbol{x}_i, \boldsymbol{y})\, \sigma(\boldsymbol{y})\, dS(\boldsymbol{y}).$$

The integrand behaves quite differently on the three different sets: On Γ_{far}, the integrand is smooth, so we simply use the standard formula $\mathbf{A}(i,j) = k(\boldsymbol{x}_i, \boldsymbol{x}_j) w_j$. On Γ_{self}, the integrand has a singularity inside the panel itself, so we have to numerically build the relevant matrix entries using a process that we will describe. On Γ_{near}, the integrand is smooth from a mathematical point of view, but its derivatives of different orders are typically large enough that the standard Gaussian quadrature rule will not be accurate, and we must again build the entries numerically. The end result will be a coefficient matrix $\mathbf{A}$ that can be decomposed as

$$\mathbf{A} = \mathbf{A}^{(\text{far})} + \mathbf{A}^{(\text{near})} + \mathbf{A}^{(\text{self})},$$

where $\mathbf{A}^{(\text{near})} + \mathbf{A}^{(\text{self})}$ is a block sparse matrix that encodes all self and near-field interactions, and $\mathbf{A}^{(\text{far})}$ represents all far field interactions. Figure 2.6 illustrates the decomposition.

Let us next describe how to build the blocks in $\mathbf{A}^{(\text{self})}$ representing self-interactions within panels. We fix a panel τ, and let I_τ and Γ_τ denote the corresponding index vector and the corresponding section of the contour, respectively. In the context of a panel based quadrature, the block $\mathbf{A}^{(\text{far})}(I_\tau, I_\tau)$ has a clear meaning, in that it represents the local action of the integral operator on the contour Γ_τ. In other words, if σ is a smooth function on Γ_τ with collocated values in the vector $\boldsymbol{\sigma}$, then the vector $\mathbf{A}^{(\text{far})}(I_\tau, I_\tau)\boldsymbol{\sigma}(I_\tau)$ should approximate the values of the local integral operator acting on σ, and evaluated at the points in Γ_τ so that

$$\mathbf{A}^{(\text{far})}(i, I_\tau)\, \boldsymbol{\sigma}(I_\tau) \approx \int_{\Gamma_\tau} k(\boldsymbol{x}_i, \boldsymbol{y}) \sigma(\boldsymbol{y})\, ds(\boldsymbol{y}), \qquad \text{for } i \in I_\tau. \tag{2.22}$$

To determine the block $\mathbf{A}^{(\text{far})}$ in practice, we enforce that (2.22) must hold exactly for all functions that correspond to polynomials up to order $p-1$ in parameter space. In other words, if $i, j \in I_\tau$, then the entry

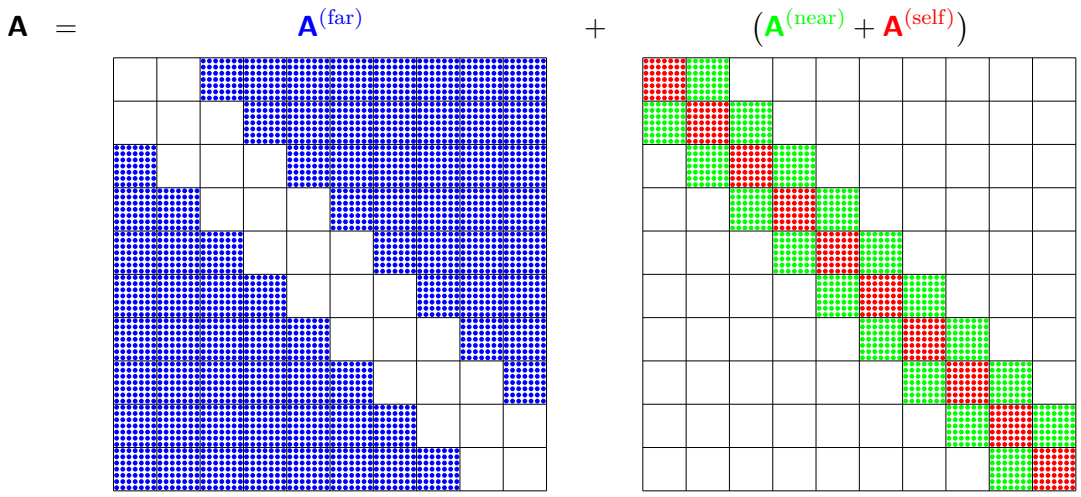

FIGURE 2.6. The matrix $\mathbf{A}$ resulting from discretization of a BIE using a panel based quadrature. Each non-zero entry in $\mathbf{A}^{(\mathrm{far})}$ is formed using the simple formula $\mathbf{A}^{(\mathrm{far})}(i,j) = k(\boldsymbol{x}_i, \boldsymbol{x}_j)w_j$. The entries in the self and near field interaction matrices $\mathbf{A}^{(\mathrm{self})}$ and $\mathbf{A}^{(\mathrm{near})}$ are computed numerically for any given contour using the technique described in Section 2.8.

$\mathbf{A}^{(\mathrm{far})}(i,j)$ is given

$$\mathbf{A}^{(\mathrm{far})}(i,j) = \int_0^1 k(\boldsymbol{x}_i, \boldsymbol{G}_\tau(t))\ell_{j'}(t)\,|\boldsymbol{G}'_\tau(t)|\,dt, \tag{2.23}$$

where $\boldsymbol{G}_\tau$ is the parameter map associated with Γ_τ, and where $\ell_{j'}$ is the Legendre interpolating polynomial on $[0,1]$ corresponding to the node $\boldsymbol{x}_j$. The integrals in (2.23) can be evaluated to any specified accuracy using specialized quadratures. The matrix $\mathbf{A}^{(\mathrm{near})}$ is also evaluated numerically in an analogous manner. We refer to [**4**] for details.

CHAPTER 3

Special topics on Integral Equations

3.1. Review of the Green identities

Recall that if $\boldsymbol{f}$ is a vector valued C^1 function on Ω, then the Gauss theorem reads

$$\int_\Omega \nabla \cdot \boldsymbol{f} = \int_\Gamma \boldsymbol{n} \cdot \boldsymbol{f},$$

where $\boldsymbol{n}$ is the outward pointing unit normal to Γ. Now suppose that u and v are two C^2 scalar value functions. Applying the Gauss theorem to $\boldsymbol{f} = u\nabla v$ and $\boldsymbol{f} = (\nabla u)v$ we find

$$\int_\Omega \big(u\,\Delta v + \nabla u \cdot \nabla v\big) = \int_\Gamma u\,\frac{\partial v}{\partial n} \tag{3.1}$$

$$\int_\Omega \big(\Delta u\, v + \nabla u \cdot \nabla v\big) = \int_\Gamma \frac{\partial u}{\partial n}\, v. \tag{3.2}$$

Subtracting (3.2) from (3.1), we find

$$\int_\Omega \big(u\,\Delta v - \Delta v\, u\big) = \int_\Gamma \left(u\,\frac{\partial v}{\partial n} - \frac{\partial u}{\partial n}\, v\right).$$

Now fix a point $x \in \Omega$ and set

$$v(y) = -\frac{1}{2\pi}\log|y - x|.$$

Further, assume u satisfies

$$-\Delta u = 0 \qquad \text{in } \Omega,$$

let ε be a small number (smaller than dist(Γ, x)), set

$$\Omega_\varepsilon = \Omega \backslash B_\varepsilon(x)$$

and observe that

$$\partial\Omega_\varepsilon = \Gamma \cup \Gamma_\varepsilon$$

where

$$\Gamma_\varepsilon = \partial B_\varepsilon(x).$$

Now note that $\Delta u(y) = \Delta v(y)$ for $y \in \Omega_\varepsilon$ to obtain

$$0 = \int_\Gamma \left(u\,\frac{\partial v}{\partial n} - \frac{\partial u}{\partial n}\, v\right) + \int_{\Gamma_\varepsilon} \left(u\,\frac{\partial v}{\partial n} - \frac{\partial u}{\partial n}\, v\right). \tag{3.3}$$

We next seek to evaluate the limit as $\varepsilon \to 0$. For $y \in \Gamma_\varepsilon$, we find

$$\begin{aligned} v(y) =& -\frac{1}{2\pi}\log|x - y| = -\frac{1}{2\pi}\log\varepsilon \\ \frac{\partial v}{\partial n}(y) =& n(y)\cdot\nabla v(y) = \frac{x-y}{|x-y|}\,\frac{x-y}{2\pi|x-y|^2} = \frac{1}{2\pi|x-y|} = \frac{1}{2\pi\varepsilon}. \end{aligned}$$

Since $u \in C(\Omega)$ we find

$$\lim_{\varepsilon\to 0}\int_{\Gamma_\varepsilon} u(y)\,\frac{\partial v}{\partial n}(y)\,dl(y) = \lim_{\varepsilon\to 0}\int_{\Gamma_\varepsilon} u(y)\,\frac{1}{2\pi\varepsilon}\,dl(y) = u(x).$$

Since $u \in C^1(\Omega)$ we know that for some finite M, we have $|\nabla u(y)| \le M$ and so

$$\lim_{\varepsilon\to 0}\left|\int_{\Gamma_\varepsilon}\frac{\partial u}{\partial n}(y)\,v(y)\,dl(y)\right| \le \limsup_{\varepsilon\to 0}\int_{\Gamma_\varepsilon} M\,\frac{1}{2\pi}\,|\log\varepsilon|\,dl(y) = \limsup_{\varepsilon\to 0} M\,\varepsilon\,|\log\varepsilon| = 0.$$

Taking the limit $\varepsilon \to 0$ in (3.3) we obtain

$$u(x) = \int_\Gamma \frac{n(y)\cdot(y-x)}{2\pi|y-x|^2}\,u(y)\,dl(y) - \int_\Gamma \frac{1}{2\pi}\log|y-x|\,u_n(y)\,dl(y). \tag{3.4}$$

We introduce two integral operators called *layer potentials* via

$$\textit{The single layer operator:} \qquad [S\,w](x) = \int_\Gamma \frac{-1}{2\pi}\log|x-y|\,w(y)\,dl(y), \tag{3.5}$$

$$\textit{The double layer operator:} \qquad [D\,w](x) = \int_\Gamma \frac{n(y)\cdot(x-y)}{2\pi|x-y|^2}\,w(y)\,dl(y). \tag{3.6}$$

Then (3.4) takes the form

$$u(x) = -[D\,u](x) + [S\,u_n](x) \qquad x\in\Omega. \tag{3.7}$$

An entirely analogous computation shows that

$$\frac{1}{2}\,u(x) = -[D\,u](x) + [S\,u_n](x) \qquad x\in\Gamma. \tag{3.8}$$

3.2. Derivation of BIEs for Laplace's equation

3.2.1. The direct formulation. We first derive a BIE for the Dirichlet problem

$$\begin{cases} -\Delta u(x) = 0, & x\in\Omega,\\ \quad u(x) = g(x), & x\in\Gamma. \end{cases}$$

From (3.8) we find that

$$\frac{1}{2}\,g(x) + [D\,g](x) = [S\,u_n](x) \qquad x\in\Gamma. \tag{3.9}$$

Equation (3.10) can be solved for the unknown boundary function u_n. Once u_n has been determined, the potential u can be recovered from (3.7).

Next consider the Neumann problem

$$\begin{cases} -\Delta u(x) = 0, & x\in\Omega,\\ \quad u_n(x) = h(x), & x\in\Gamma. \end{cases}$$

From (3.8) we find that

$$\frac{1}{2}\,u(x) + [D\,u](x) = [S\,h](x) \qquad x\in\Gamma. \tag{3.10}$$

Equation (3.10) can be solved for the unknown boundary function $u|_\Gamma$. Once $u|_\Gamma$ has been determined, the potential u can be recovered from (3.7).

3.3. Problems with body loads

Integral equation formulations are as we have seen particularly compelling for problems where data is prescribed only on the boundary of a computational domain, since they in this situation allows us to formulate an equation that itself lives only on the boundary. But integral equation formulations can also be useful for many problems involving body loads. The idea is to follow a classical method of splitting the problem into two parts: First a particular solution that satisfies the PDE but not the boundary condition is determined, and then a homogeneous solution that corrects the boundary condition is determined using the ideas described earlier in this chapter. However, some numerical complications may arise, as we will discuss.

Let us consider a general boundary value problem involving a body load

$$Au = h, \qquad \text{on } \Omega, \tag{3.11}$$

$$u = f \qquad \text{on } \Gamma, \tag{3.12}$$

where Ω is a domain in $\mathbb{R}^2$ with boundary Γ, where h is a given body load, and where f is given Dirichlet boundary data. The first step is to construct a "particular solution", $u_{\rm p}$, with the property that

$$Au_{\rm p} = h, \qquad \text{on } \Omega.$$

Setting $u_{\rm h} = u - u_{\rm p}$, we find that $u_{\rm h}$ satisfies

$$Au_{\rm h} = 0, \qquad \text{on } \Omega,$$

$$u_{\rm h} = f, \qquad \text{on } \Gamma.$$

Since $u_{\rm h}$ satisfies a homogeneous problem, it can be determined using the boundary integral technique described in Sections 1.1 — 1.5.

Now, if Ω is a rectangle (or some other simple geometrical shape), and if h is a smooth function on h, then one can easily compute a particular solution $u_{\rm p}$ by integrating against the fundamental solution of the free space problem

$$u_{\rm p}(\boldsymbol{x}) = \int_{\Omega} \phi(\boldsymbol{x} - \boldsymbol{y})\, h(\boldsymbol{y})\, dA(\boldsymbol{y}).$$

When h is smooth, but Ω is not a simple geometric shape, it may be easier to compute an integral over some extension $\Omega_{\rm big}$ of Ω,

$$u_{\rm p}(\boldsymbol{x}) = \int_{\Omega_{\rm big}} \phi(\boldsymbol{x} - \boldsymbol{y})\, h_{\rm big}(\boldsymbol{y})\, dA(\boldsymbol{y}),$$

where $h_{\rm big}$ is a smooth extension of h from Ω to $\Omega_{\rm big}$, see [?]. Another alternative, which is attractive when h is not easily integrable, is to use the FFT or some other fast Poisson solver so solve the equation

$$Au_{\rm p} = h \qquad \text{on } \Omega_{\rm big}.$$

3.4. Variable coefficient PDEs and the Lippmann-Schwinger equation

3.5. BIEs for different elliptic PDEs

Bibliography

[1] Bradley K Alpert, *Hybrid Gauss-trapezoidal quadrature rules*, SIAM Journal on Scientific Computing **20** (1999), no. 5, 1551–1584.

[2] James Bremer, *On the nyström discretization of integral equations on planar curves with corners*, Applied and Computational Harmonic Analysis **32** (2012), no. 1, 45–64.

[3] A. Gillman, S. Hao, and P.G. Martinsson, *A simplified technique for the efficient and highly accurate discretization of boundary integral equations in 2d on domains with corners*, Journal of Computational Physics **256** (2014), no. 0, 214 – 219.

[4] S. Hao, A.H. Barnett, P.G. Martinsson, and P. Young, *High-order accurate methods for nyström discretization of integral equations on smooth curves in the plane*, Advances in Computational Mathematics **40** (2014), no. 1, 245–272 (English).

[5] J. Helsing and R. Ojala, *Corner singularities for elliptic problems: Integral equations, graded meshes, quadrature, and compressed inverse preconditioning*, Journal of Computational Physics **227** (2008), no. 20, 8820 – 8840.

[6] Sharad Kapur and Vladimir Rokhlin, *High-order corrected trapezoidal quadrature rules for singular functions*, SIAM Journal on Numerical Analysis **34** (1997), no. 4, 1331–1356.

[7] Rainer Kress, *Linear integral equations*, second ed., Applied Mathematical Sciences, vol. 82, Springer, 1999.

[8] William McLean, *Strongly elliptic systems and boundary integral equations*, Cambridge University Press, Cambridge, 2000. MR 2001a:35051

[9] Kirill Serkh and Vladimir Rokhlin, *On the solution of elliptic partial differential equations on regions with corners*, Journal of Computational Physics **305** (2016), 150 – 171.